

# Light Scattering Study of Semidilute Aqueous Systems of Chitosan and Hydrophobically Modified Chitosans

Anna-Lena Kjøniksen,<sup>†</sup> Christian Iversen,<sup>†</sup> Bo Nyström,<sup>\*,†</sup> Torgeir Nakken,<sup>‡</sup> and Odd Palmgren<sup>‡</sup>

Department of Chemistry, University of Oslo, P.O. Box 1033, Blindern, N-0315 Oslo, Norway, and Norsk Hydro, Research Centre Porsgrunn, Department of Polymer and Surface Chemistry, P.O. Box 2560, N-3901, Porsgrunn, Norway

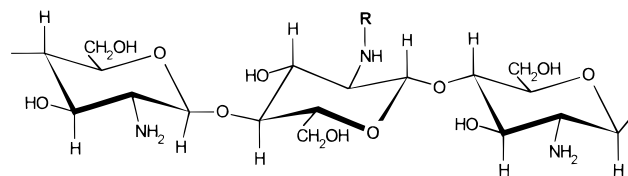
Received May 26, 1998; Revised Manuscript Received September 15, 1998

**ABSTRACT:** Intensity (ILS) and dynamic light scattering (DLS) experiments were performed on semidilute acid aqueous solutions of unmodified chitosan (UM-chitosan) and of hydrophobically modified chitosan (HM-chitosan) with two different degrees of C12-aldehyde substitution. Both the ILS and the DLS measurements suggest the formation of association structures. According to the ILS measurements in the range  $q\xi > 1$  ( $q$  is the wave vector and  $\xi$  is the correlation length), all the systems have a fractal structure and the fractal dimension is about 2. The time correlation data obtained from the DLS experiments revealed, for all systems, the existence of two relaxation modes, one single exponential at short times followed by a stretched exponential at longer times. The value of the slow relaxation time increases with increasing concentration and hydrophobicity. This behavior reflects the importance of intermolecular associations and hydrophobic interactions. The reduced slow relaxation time exhibits a weak temperature dependence for both UM-chitosan and HM-chitosans. The fast mode is always diffusive, while the slow mode shows an approximately  $q^3$  dependence at low concentrations and a  $q^2$  dependence, characteristic of diffusion, at higher concentrations.

## Introduction

Over the past few years, many studies have been devoted to hydrophobically modified water soluble polysaccharides, i.e., polysaccharides with low levels of hydrophobic groups.<sup>1–8</sup> Upon a certain polymer concentration, these materials exhibit much higher viscosities<sup>4,6</sup> in aqueous solutions than the corresponding unmodified polymers because the contact between the hydrophobic moieties and water is energetically unfavorable, so that the hydrophobically modified polymers have a strong tendency to associate. These polymers have found importance in various biomedical and pharmaceutical applications. Because of this amphiphilic behavior, hydrophobically modified polymers are also called “associative thickeners” and they may act, even at low concentration, as powerful rheology modifiers so that they can be used in various industrial applications where the control of the rheology of the solution is required: paints, foods, pharmaceuticals, enhanced oil recovery, etc. Recent studies have shown that these systems can be used as matrixes for immobilization of enzymes and drugs, and as support materials for hydrophobic chromatography.<sup>9</sup>

We have recently studied<sup>10–12</sup> the rheological properties of aqueous systems of unmodified chitosan (UM-chitosan) and its hydrophobically modified analogues (HM-chitosan). The rheological features of these systems, as well as some preliminary light scattering results, have recently been reviewed.<sup>13</sup> The polysaccharide chitosan<sup>14</sup> belongs to a family of linear cationic biopolymers obtained from alkaline *N*-deacetylation of chitin, which is the second most abundant polymer in nature. Chitosan is a random copolymer, containing (1→4) linked 2-acetamido-2-deoxy- $\beta$ -D-glucopyranose



Chitosan:  $R = H$  or  $R = -CO-CH_3$

HM-Chitosan:  $R = H$  or  $R = C12$ -aldehyde or  $R = -CO-CH_3$

**Figure 1.** Schematic illustration of the structure of unmodified chitosan (UM-chitosan) and the hydrophobically modified chitosan (HM-chitosan).

and 2-amino-2-deoxy- $\beta$ -D-glucopyranose units. A schematic illustration of the structure of chitosan is displayed in Figure 1. At acidic pH, chitosan is water-soluble and due to the presence of protonated amino groups it exhibits a polyelectrolyte character at low pH. The physical properties of aqueous systems of chitosan have attracted a great deal of interest, and different experimental techniques have been applied in these studies. Effects such as pH, ionic strength, polymer concentration, temperature, degree of deacetylation, and hydrophobicity of the polymer on the physical behavior of chitosan systems have been investigated.<sup>15–30</sup> Most of these papers are concerned with structural<sup>15,17,19,21,22,25,27</sup> and rheological<sup>16,18,20,22,30</sup> properties of systems of unmodified chitosan. However, there is a lack of studies dealing with the structure and dynamics of semidilute solutions of UM-chitosan and HM-chitosan.

In this paper, we report results from intensity light scattering (ILS) and dynamic light scattering (DLS) measurements of semidilute solutions of UM-chitosan and HM-chitosan (two different degrees of hydrophobicity) at different temperatures. The aim of this work is to gain a deeper insight into how the polymer concentration and the hydrophobicity of the polymer affect the structural characteristics and the dynamical behavior

<sup>†</sup> University of Oslo.

<sup>‡</sup> Research Centre Porsgrunn.

of chitosan systems. Furthermore, some aspects on the influence of temperature on the dynamic properties will be given.

## Experimental Section

**Materials and Solution Preparation.** The unmodified chitosan sample was obtained from Pronova Biopolymers (Drammen, Norway). The degree of deacetylation was determined to be 84% by  $^1\text{H}$  NMR spectroscopy<sup>31</sup> and by using low-angle laser light scattering (LALLS) and size-exclusion chromatography (SEC) the weight-average molecular weight  $M_w$  was found to be  $4 \times 10^5$  and the polydispersity index  $M_w/M_n$  was 2.7. The details of these methods used in the characterization of chitosan have been given elsewhere.<sup>28</sup>

The hydrophobically modified samples were prepared by reaction with the amino groups of the backbone of the polymer chain with C12-aldehyde. Except for the C12-aldehyde substitution the modified samples are equivalent to their unmodified analogue. The modification procedure employed here is similar to the methods described earlier.<sup>32</sup> The degrees of C12-aldehyde substitution used in this work are 2.5 and 5 mol %. Aqueous samples of UM-chitosan and HM-chitosans in 1% acetic acid were prepared by weighing the components and allowing the solutions to homogenize by stirring at room temperature for 3 days. All the measurements reported in this paper have been carried out in the semidilute concentration regime, as defined below, where intermolecular associations are expected to prevail. The onset of this regime can be estimated from the overlap concentration  $c^* = 1/[\eta]$ , where  $[\eta]$  is the intrinsic viscosity. From intrinsic viscosity data<sup>11</sup> for the UM-chitosan and HM-chitosan systems, the values of  $c^*$  were determined<sup>12</sup> to be 0.04 and 0.03, respectively. Solutions with concentrations of 0.1, 0.25, 0.50, 0.75, and 1.0 wt % were prepared. All the measurements were carried out at pH  $\approx$  3.8, the value that was obtained in this polymer concentration range by dissolving chitosan or HM-chitosan in 1% acetic acid. The solutions were filtered in an atmosphere of filtered air through 0.8  $\mu\text{m}$  filters (Micro Filtration Systems) directly into precleaned 10 mm NMR tubes (Wilma Glass Co.) of highest quality.

**Light Scattering Experiments.** The scattering process allows us to explore a system on a length scale of  $q^{-1}$ , where  $q$  is the wave vector defined as  $q = 4\pi n \sin(\theta/2)/\lambda$ . Here  $\lambda$  is the wavelength of the incident light in a vacuum,  $\theta$  is the scattering angle, and  $n$  is the refractive index of the solution. The value of  $n$  was determined at each temperature and concentration at  $\lambda = 488$  nm by using an Abbé refractometer.

The light scattering measurements were carried out on a standard laboratory built light scattering spectrometer capable of doing both absolute integrated scattering intensity and photon correlation experiments at different scattering angles. A Spectra Physics Model 2020 argon ion laser operating at a wavelength of 488 nm was used. The light was vertically polarized and the intensity of the output beam was adjusted with the aid of high quality neutral density filters (Melles Griot) of various transmittances depending upon the intensity of the scattered light from the sample solutions. To ensure vv configuration, polarizers were used both in front and behind the cell. The sample cell was held in a thermostat block filled with refractive index matching dibutyl phthalate, the temperature constancy being controlled to within  $\pm 0.05$  °C.

The intensity light scattering (ILS) experiments were conducted using ALV (Langen-Germany) light scattering electronics in combination with the on-line program ODIL.

In the present experimental configuration a detection geometry was used where a vertical slit, instead of a pinhole, is placed in front of the photomultiplier tube. With this arrangement, the absolute quantity  $R_{vv}(q) = hI^*(q)$ , where  $I^*(q)$  is the excess scattered intensity and  $h = R_{vv,\text{benzene}}I_{\text{solv}}/(I^*_{\text{benzene}}I_{\text{benzene}})$ . A value of  $R_{vv}(90^\circ) = 3.14 \times 10^{-5} \text{ cm}^{-1}$  reported<sup>33</sup> for benzene at 25 °C and 488 nm was employed in this study. The optical constant  $K (\text{cm}^3 \text{ mol g}^{-2})$  was calculated from  $K = (4\pi^2 n^2/N_A \lambda^4)(\partial n/\partial c)^2$ , where  $N_A$  is Avogadro's constant,  $(\partial n/\partial c)$  is the refractive index increment, and  $c$  is the mass

concentration (mass/volume). The values of the refractive index increment used in this work were taken from previously published data<sup>26</sup> for chitosan solutions in weakly acetic acid. The reduced scattered intensity,  $Kc/R_{vv}(q)$  was calculated and values of this quantity in the limit  $q = 0$  were determined from a Guinier plot,<sup>34</sup> that is, a plot of  $\ln(Kc/R_{vv}(q))$  versus  $q^2$ .

In the DLS experiments, the full homodyne intensity autocorrelation function was determined with the aid of an ALV-5000 multiple- $\tau$ -digital correlator. The correlation functions were recorded in the real time "multiple- $\tau$ " mode of the correlator, in which 256 time channels are logarithmically spaced over an interval ranging from 0.2  $\mu\text{s}$  to almost 1 h.

If the scattered field is assumed to have Gaussian statistics, the experimentally determined homodyne intensity autocorrelation function  $g^{(2)}(q, t)$  is directly related to the theoretically amenable first-order electric field autocorrelation function  $g^{(1)}(q, t)$ , through the Siegert<sup>35</sup> expression  $g^{(2)}(q, t) = 1 + B|g^{(1)}(q, t)|^2$ , where  $B (\leq 1)$  is an instrumental parameter.

In this study, as well as in other DLS studies<sup>6,36–40</sup> on associating systems, the decay of the correlation function has been found to initially be described by a single exponential, followed at longer times by a stretched exponential

$$g^{(1)}(t) = A_f \exp(-t/\tau_f) + A_s \exp[-(t/\tau_{se})^\beta] \quad (1)$$

with  $A_f + A_s = 1$ . The parameters  $A_f$  and  $A_s$  are the amplitudes for the fast and the slow relaxation modes, respectively. When time correlation functions from DLS at long wavelengths in the semidilute regime are analyzed, the first term (short-time behavior) on the right-hand side of eq 1 yields the cooperative diffusion coefficient  $D_c$  ( $\tau_f^{-1} = D_c q^2$ ), which reflects a concerted motion of polymer chains relative to the solvent. The second term (long-time behavior) is expected to be associated with disengagement relaxation of individual chains<sup>37,41</sup> or cluster relaxation.<sup>42</sup> The variable  $\tau_{se}$  is some effective relaxation time, and  $\beta$  ( $0 < \beta \leq 1$ ) is a measure of the width of the distribution of relaxation times. The distribution of relaxation times for the present systems is rather narrow with  $\beta = 0.8–0.9$ . The  $\beta$  variable has been interpreted<sup>41</sup> as a measure of inhomogeneity or disorder effects of the system and the specific value of  $\beta$  depends on the topological dimension of the modeled cluster. In the coupling model of Ngai,<sup>42</sup> the value of the stretch exponent  $\beta$  is a direct measure of the coupling strength of the relaxation mode to its complex environments. At short times, the relaxation process is not affected by coupling effects, but at long times dynamical constraints come into play and give rise to a fractional decay of the relaxation function. In view of eq 1, the mean relaxation time is given by

$$\tau_s \equiv \int_0^\infty \exp[-(t/\tau_{se})^\beta] dt = (\tau_{se}/\beta)\Gamma(1/\beta) \quad (2)$$

where  $\Gamma(1/\beta)$  is the gamma function.

In the analysis of correlation function data, a nonlinear fitting algorithm (a modified Levenberg–Marquardt method) was employed to obtain best-fit values of the parameters  $A_f$ ,  $\tau_f$ ,  $\tau_{se}$ , and  $\beta$  appearing on the right-hand side of eq 1.

## Results and Discussion

**Intensity Light Scattering.** The features of the light scattered by polymer solutions depend on the concentration regime and on the relative magnitude of the characteristic length scale probed in the light scattering experiment. In semidilute solutions (as in this work), i.e., above the concentration  $c^*$  where the polymer chains begin to overlap, the characteristic length is the correlation or screening length  $\xi$  that decreases with increasing polymer concentration. In this concentration regime the solution can be visualized as a transient network with a certain average mesh size  $\xi$ .<sup>43</sup>

In the Guinier region ( $q\xi < 1$ ), the angular distribution of scattered intensity is observed and the normal-

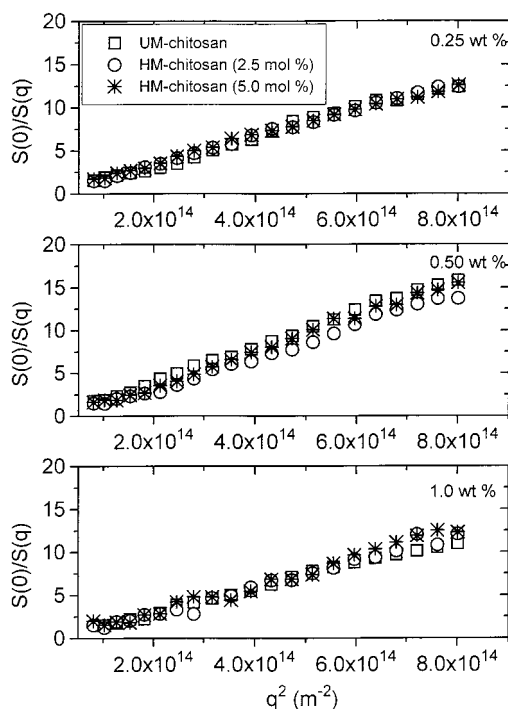


**Figure 2.**  $q^2$  dependence of the reduced inverse scattered intensity function for the polymers and concentrations indicated.

ized inverse scattered intensity function can be described by a Ornstein–Zernike law<sup>43</sup>

$$S(0)/S(q) = 1 + q^2 \xi^2 \quad (3)$$

where  $S(q) = R_w(q)/KcM$  and  $S(0) = RT/M(\partial\pi/\partial c)$ , with  $R$  the gas constant,  $T$  the temperature, and  $(\partial\pi/\partial c)$  the inverse osmotic compressibility.

The angular dependence of the reciprocal normalized scattering intensity, depicted in Figure 2 for solutions of UM-chitosan and HM-chitosans of different concentrations, is fairly strong, suggesting the existence of light scatters with large dimensions. We can see that the solutions of UM-chitosan and HM-chitosans exhibit practically the same angular dependence for the considered concentrations.

By plotting the inverse of the scattered intensity function as a function of  $q^2$  at small scattering angles, the quantity  $\xi$  can be determined with the aid of eq 3. Effects of concentration and hydrophobicity on  $\xi$  are displayed in Figure 3. At moderate concentrations in the semidilute regime, the value of  $\xi$  is practically independent of concentration and it is higher for UM-chitosan. This indicates that the average mesh size of the UM-chitosan network is larger than the corresponding ones for the networks of the HM-chitosans. At higher concentrations the correlation length gradually declines, which is consistent with the predicted feature of  $\xi$ , and it seems that at the highest concentration the mesh size is virtually independent of the degree of hydrophobicity. The relatively weak concentration dependence of  $\xi$  may indicate that only a limited part of the semidilute regime is covered by these concentrations and that the thermodynamic conditions of the systems are marginal or moderately good.

In the regime  $q\xi > 1$ , the length scale  $q^{-1}$  is associated with more local properties of the system (one sees inside of the clusters) and the scattered intensity depends strongly on the length scale. A semidilute solution can

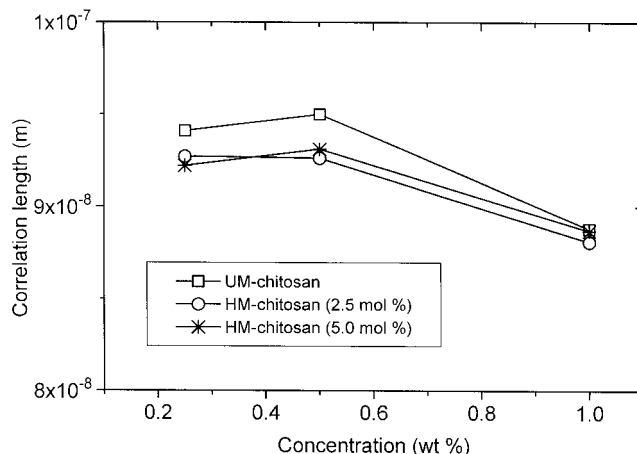


**Figure 3.** Effects of polymer concentration and hydrophobicity on the correlation length of the systems indicated. The solid curves are only guides for the eye.

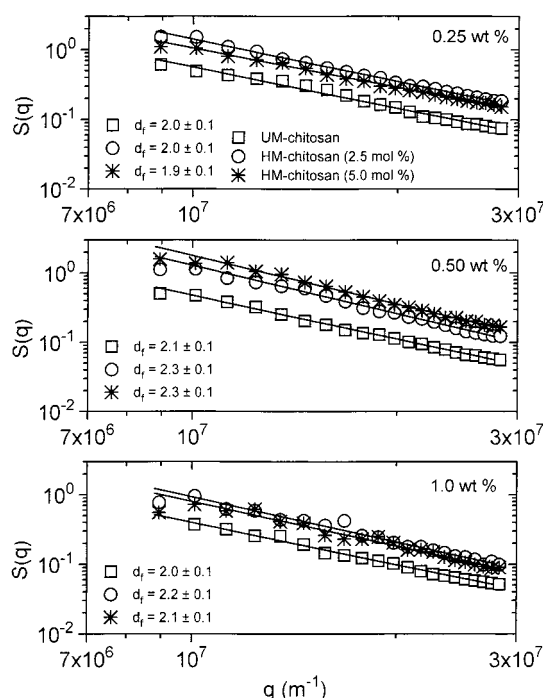


**Figure 4.** log–log plot of the scattered intensity function for the systems indicated. The solid lines represent the best fits of the experimental data (see eq 4).

be viewed as an irregular fractal network,<sup>44</sup> formed by more or less interpenetrating clusters. In the “intermediate  $q$  regime” ( $q\xi > 1$ ), the scattering experiment probes the internal structure of the polymers and the scattered intensity or the structure factor decays with the wave vector as

$$S(q) \sim q^{-d_f} \quad (4)$$

where the slope of the structure factor in the power-law regime yields the fractal dimension  $d_f$ . The value of  $d_f = 5/3$  is for the excluded volume regime and  $d_f = 2$  for a Gaussian chain.<sup>45</sup>

Figure 4 shows the intensity profiles in form of log–log plots of  $S(q)$  versus  $q$  for semidilute solutions of UM-chitosan and HM-chitosans. The solid lines represent the best fit of the experimental data with eq 4. The values of  $d_f$  are approximately 2, virtually independent of polymer concentration and hydrophobicity. The



fractal dimension is related to the Flory excluded volume exponent  $\nu$  ( $R_G \sim M^\nu$ , where  $R_G$  is the radius of gyration) through the expression  $d_f = 1/\nu$ , where  $\nu$  assumes values of 3/5 and 1/2 for good and  $\Theta$  solvents, respectively. The observed value of  $d_f \approx 2$  is compatible with the values of  $\nu$  around 0.5 that can be inferred from ILS measurements<sup>17,22,25</sup> on dilute acidic solutions of chitosan. However, a comparison of the present results with those obtained from other systems is intricate because the degree of deacetylation and the used solvent will have a significant influence on the physical properties of the chitosan solutions.

In a previous paper<sup>12</sup> the fractal dimensions at the gel points of UM-chitosan and HM-chitosans were determined from oscillatory shear measurements by employing the theoretical approach of Muthukumar.<sup>46</sup> The values of  $d_f$  were found to be 2.2 and 2.0 for incipient gels of UM-chitosan and HM-chitosans, respectively, and these values are close to those observed from the present ILS study. However, in contrast to the values of  $d_f$  from the rheological experiments, the values of  $d_f$  from ILS did not reveal any structural difference between UM-chitosan and HM-chitosans. The reason for this may be that the concentrations utilized in ILS are far below the concentrations for the formation of incipient gels. We may note that these values of  $d_f$  are significantly higher than that (1.3) reported<sup>19</sup> from a small-angle X-ray scattering investigation on 2 wt % acetic acid aqueous solutions of chitosan with a degree of deacetylation of 79% (the degree of acetylation of the present samples is 84%). The reason for this difference in fractal dimension is not clear, but it was observed that the degree of deacetylation has a strong influence on the heterogeneity of the chitosan sample.

A universal representation of the ILS data<sup>47</sup> can be displayed by plotting the reduced scattered intensity function ( $S(q\xi)/S(0)$ ) as a function of the reduced length scale  $q\xi$  (dimensionless quantity). By this procedure the experimental points will condense onto a single curve (see Figure 5). This plot should be independent of the chemical nature of the polymer, its molecular mass, and its concentration. This type of representation constitutes a manifestation of the self-similarity of the polymer conformations, which is preserved at length scales smaller than  $\xi$  in semidilute polymer solutions. The straight lines ( $d_f = 2.0$ ) represent the power law behavior at  $q\xi > 1$ .

**Dynamic Light Scattering.** In Figure 6, normalized time correlation data for aqueous UM-chitosan and HM-chitosan solutions of various concentration, together with the corresponding curves fitted by means of eq 1, are depicted in the form of semilogarithmic plots. A comparison of the correlation functions clearly reveals that there is, for both the unmodified and hydrophobically modified chitosan, a progressive slowing down of the relaxation process as the concentration increases. As a result of specific hydrophobic associations, this effect is more pronounced for the HM-chitosan solutions. The slowing down tendency of the relaxation process probably reflects that an increase in concentration promotes enhanced association effects. The conjecture is that these features impose dynamical constraints on the system, and as a result the relaxation of the correlation function is delayed. We should note that the appearance of a slow relaxation mode in the profile of the correlation function is a common feature that has been reported<sup>48–50</sup> for many semidilute polyelectrolyte

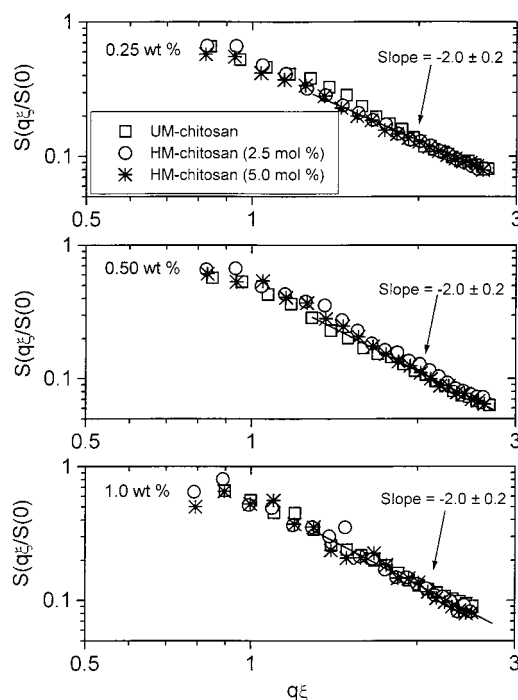


**Figure 5.** Plot of the quantity  $S(q\xi)/S(0)$  as a function of the dimensionless scaling variable  $q\xi$  for the systems and concentrations indicated. The solid lines indicate the scaling behavior at  $q\xi > 1$ .

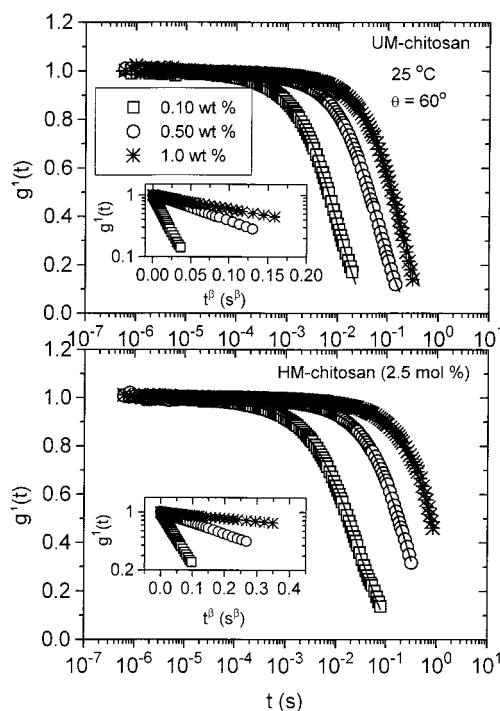


**Figure 6.** Plot of the first-order field correlation function versus time (every second point is shown) for the displayed systems at the scattering angle, temperature, and concentrations indicated. The solid curves are fitted with the aid of eq 1. The inset plots demonstrate the stretched exponential character of the correlation function at long time.

systems. This mode is usually associated with aggregates or multichain domains. The inset plots show semilogarithmic plots of  $g^1(t)$  as a function of  $t^{1/2}$ . This type of plot yields straight lines for functions that can be represented by stretched exponentials. It is observed that, within experimental error, the long time behaviors

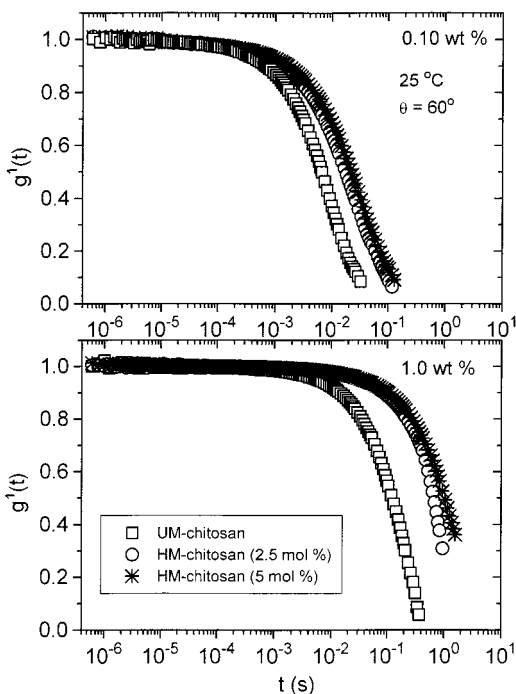


**Figure 7.** Effect of hydrophobicity on the correlation functions (every second point is shown) at the scattering angle, temperature, and concentrations indicated.

of the correlation functions are well described by straight lines.

The effect of hydrophobicity on the time correlation functions is depicted in Figure 7 for two different polymer concentrations (0.1 and 1.0 wt %). It is evident that the decay time is shifted toward higher values when the degree of hydrophobic substitution is raised from 0 to 2.5 mol %, and this effect is enhanced with increasing polymer concentration. We should note that when the hydrophobic substitution is increased from 2.5 to 5 mol %, there is only a small additional shift of the correlation function.

The influence of temperature on the time correlation function for UM-chitosan and HM-chitosans at a concentration of 0.5 wt % is illustrated in Figure 8. In this plot, trivial temperature and solvent viscosity effects on the decay of the correlation function have been eliminated by introducing the reduced quantity ( $tT/\eta_0$ ) on the x-axis. Here  $\eta_0$  is the solvent viscosity and  $T$  is the absolute temperature. Despite this normalization, we observe that the long-time tail of the correlation function is shifted toward longer times with decreasing temperature.

In the analysis of the correlation functions with the aid of eq 1, a number of characteristic parameters can be extracted. From the fast inverse relaxation time ( $\tau_f^{-1} = D_c q^2$ ) the cooperative diffusion coefficient can be determined. The temperature dependence of the reduced cooperative diffusion coefficient,  $D_c \eta_0 / T$ , for 1 wt % solutions of UM-chitosan and HM-chitosans is shown in Figure 9a. The results show that the reduced diffusion coefficient drops with increasing temperature for both the UM-chitosan and the HM-chitosans, and the values of the diffusion coefficient seem to be higher for the hydrophobically modified samples. A similar temperature dependence of the diffusion quantity is also observed for the other polymer concentrations. This behavior may be related to an increased flexibility<sup>29</sup> of the polymer chains with increasing temperature.

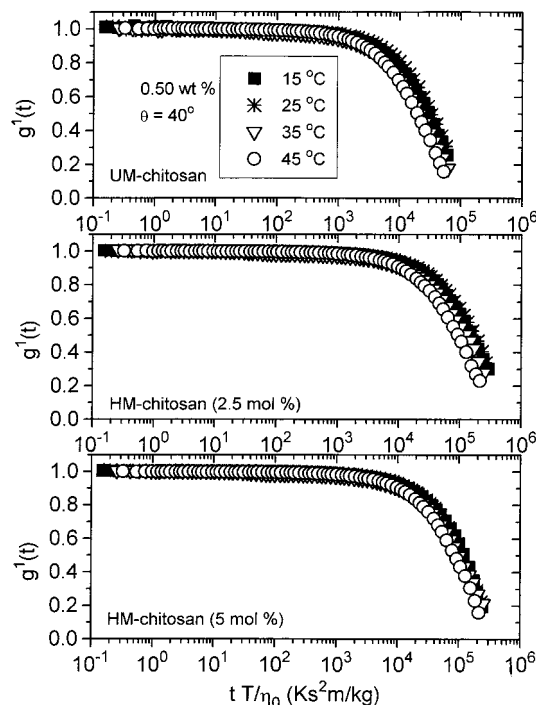


**Figure 8.** Plot of the first-order field correlation function versus the reduced variable  $tT/\eta_0$  (every second point is shown) for the displayed systems at the scattering angle, temperatures, and concentration indicated.

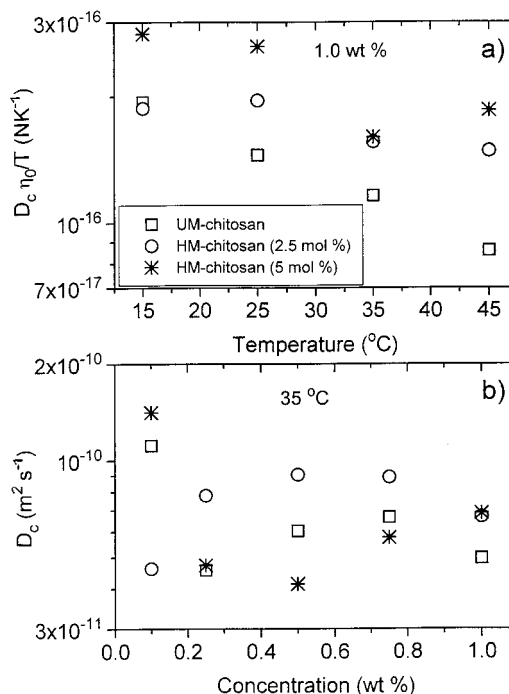


**Figure 9.** (a) Temperature dependence of the reduced cooperative diffusion coefficient for the systems and concentration indicated. (b) Concentration dependence of the cooperative diffusion coefficient for the systems and the temperature indicated.

The concentration dependence of  $D_c$  at 35 °C (the same behavior is also found at the other temperatures) for UM-chitosan and HM-chitosans is depicted in Figure 9b. In view of the fairly large scatter in the diffusion data, it is difficult to establish a specific trend, but the general picture that emerges is that  $D_c$  is virtually independent of concentration in the considered regime. The reason for the large scatter is probably that the

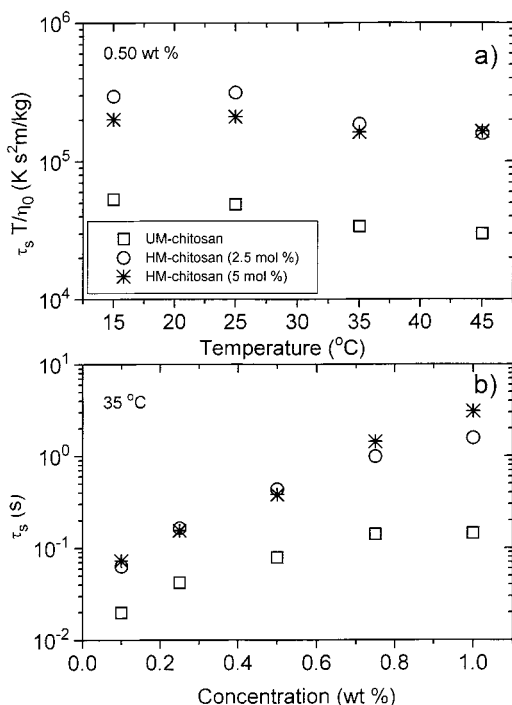


**Figure 10.** (a) Temperature dependence of the reduced slow relaxation time for the systems and concentration indicated. (b) Concentration dependence of the slow relaxation time for the systems and the temperature indicated.

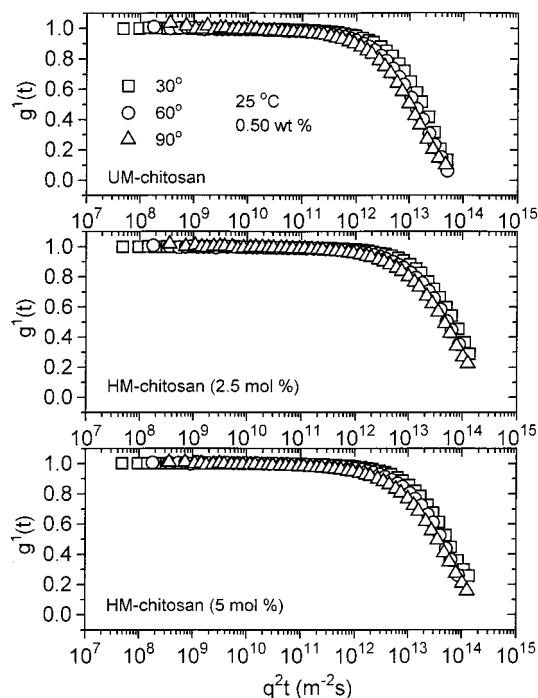


**Figure 11.** Plot of the first-order field correlation function versus  $q^2t$  (every third point is shown) for the displayed systems at the scattering angles, temperature, and concentration indicated.

contribution of the fast mode to the decay is small and therefore difficult to extract with great accuracy. A weak concentration dependence of  $D_c$  may indicate that the thermodynamic conditions of the system are moderately good and that a restricted part of the semidilute regime is covered.

The slow relaxation time  $\tau_s$  is another parameter that can be calculated with the aid of the model relationship

(eq 1) in combination with eq 2. Figure 10a shows the effect of temperature on the reduced slow relaxation time ( $\tau_s T/\eta_0$ ) for 0.5 wt % solutions of UM-chitosan and HM-chitosans. The values of the reduced quantity are higher for the HM-chitosan solutions than for the corresponding solutions of UM-chitosan. This probably reflects the effect of the hydrophobic associations. For both the unmodified and the hydrophobically modified samples, the results indicate a weak decrease of the reduced relaxation time with increasing temperature. This trend may be due to the increased mobility of the polymer chains that disrupts intermolecular associations as the temperature increases. In this context, it is interesting to note that a similar temperature dependence of the dynamic viscosity has recently been reported<sup>13</sup> for the same chitosan systems. The dynamic viscosity is, in a similar way as the slow relaxation time, associated with chain disengagement relaxation. In a recent rheological study<sup>30</sup> of semidilute chitosan solutions it was argued that the solubility of chitosan is improved at higher temperatures.

The effects of concentration and hydrophobicity on the slow relaxation time for solutions of UM-chitosan and HM-chitosan at 35 °C (a similar behavior is also observed at the other temperatures) are illustrated in Figure 10b. It is evident that the slow relaxation time increases strongly with concentration, and the values of  $\tau_s$  are consistently higher for the HM-chitosans than for the UM-chitosan. This tendency seems to become more pronounced at higher concentrations. These findings suggest that increased polymer concentration and hydrophobicity promote interpolymer association, and thereby slow the process of chain or cluster disengagement. It is reasonable to assume that the rise of  $\tau_s$  with concentration for the unmodified chitosan sample can to a large extent be traced to enhanced intermolecular interactions. However, the results from a recent fluorescence study<sup>27</sup> of aqueous solutions of unmodified chitosan have indicated that the hydrophobicity raises with increasing concentration and that chitosan chains are self-associated<sup>25,27,28</sup> by intermolecular hydrophobic interactions. In this context, we may note that the concentration dependences of the slow relaxation time for UM-chitosan and HM-chitosans are reminiscent of the behaviors observed<sup>12</sup> from zero-shear viscosity results of the same systems. This method is also associated with the disengagement of chains or clusters.

The angular dependence of the correlation function, at a concentration of 0.5 wt % and at different hydrophobicities, is displayed in the form of a reduced plot in Figure 11. The fast mode is diffusive, while the separation of the curves at longer times suggests that the slow mode exhibits a stronger  $q$  dependence. This type of behavior of the slow relaxation mode is frequently observed for associating systems.<sup>6,38,39,51–53</sup> The  $q$  dependence of the inverse slow relaxation time may be expressed as  $\tau_s^{-1} \sim q^\alpha$ . The general trend, both for UM-chitosan and HM-chitosan, is that  $\alpha_s$  falls off from ca. 2.6 to 2 (diffusive motion) as the concentration increases (see Figure 12) from 0.1 to 1 wt %. Since the screening length (or mesh size) drops with concentration (see Figure 3), our conjecture is that the decrease of  $\alpha_s$  reflects crossover effects in connection with the transition from the regime  $q\xi > 1$  to the global regime  $q\xi < 1$ , characteristic of diffusion.



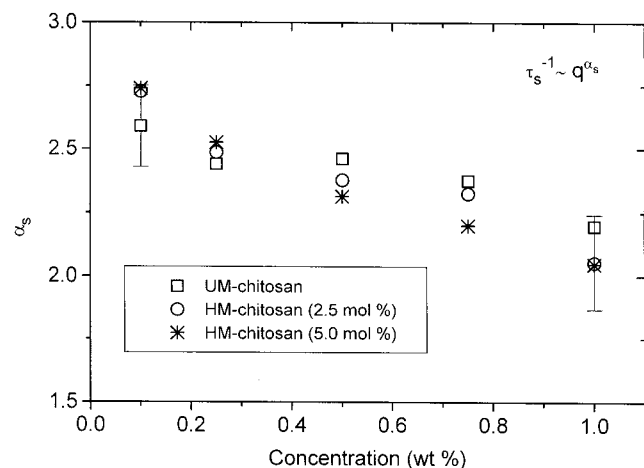


**Figure 12.** Effect of polymer concentration on the power law exponent  $\alpha_s$ , illustrating the  $q$  dependence of the slow inverse relaxation time for the systems indicated.

## Conclusions

In summary, through intensity and dynamic light scattering we have characterized the static and dynamic properties of semidilute aqueous solutions of chitosan and of hydrophobically modified analogues. The excess scattering at low angles, as well as the pronounced shift in the decay time toward higher values with increasing polymer concentration and hydrophobicity suggests the formation of association structures. The intensity light scattering measurements revealed in the regime  $q\xi > 1$  a power law in the form  $S(q) \sim q^{-d}$ , with a fractal dimension of about 2 for all the systems.

The DLS results show that the slow relaxation time, associated with chain disengagement relaxation, raises with increasing polymer concentration and hydrophobicity. The reason for this behavior can probably be attributed to enhanced intermolecular interactions and hydrophobic interactions. The reduced slow relaxation time decreases with increasing temperature, which probably is due to enhanced mobility of the chains. The fast relaxation mode is always diffusive, while the slow relaxation mode exhibits a stronger  $q$  dependence at low concentrations but becomes diffusive at high concentrations. This behavior is practically the same, independent of the hydrophobicity of the sample.

**Acknowledgment.** This work was supported by Norsk Hydro and the Norwegian Research Council through the program PROSMAT.

## References and Notes

- (1) *Macromolecular Complexes in Chemistry and Biology*, Dubin, P., Bock, J., Davies, R. M., Schulz, D. N., Ties, C., Eds.; Springer-Verlag: Berlin, 1994.
- (2) Gelman, R. A. Hydrophobically modified hydroxyethylcellulose. TAPPI International Dissolving Pulps Conference, Geneva, Switzerland, 1987.
- (3) Zugenmaier, P.; Aust, N. *Makromol. Chem. Rapid Commun.* **1990**, *11*, 95.
- (4) Tanaka, R.; Meadows, J.; Williams, P. A.; Phillips, G. O. *Macromolecules* **1992**, *25*, 1304.
- (5) Guillemet, F.; Piculell, L. *J. Phys. Chem.* **1995**, *99*, 9201.
- (6) Nyström, B.; Thuresson, K.; Lindman, B. *Langmuir* **1995**, *11*, 1994.
- (7) Thuresson, K.; Nyström, B.; Wang, G.; Lindman, B. *Langmuir* **1995**, *11*, 1, 3730.
- (8) Thuresson, K.; Söderman, O.; Hansson, P.; Wang, G. *J. Phys. Chem.* **1996**, *100*, 4909.
- (9) Akiyoshi, K.; Deguchi, S.; Moriguchi, N.; Yamaguchi, S.; Sunamoto, J. *Macromolecules* **1993**, *26*, 3062.
- (10) Kjøniksen, A.-L.; Nyström, B.; Nakken, T.; Palmgren, O.; Tande, T. *Polym. Bull.* **1997**, *38*, 71.
- (11) Kjøniksen, A.-L.; Nyström, B.; Iversen, C.; Nakken, T.; Palmgren, O.; Tande, T. *Langmuir* **1997**, *13*, 4948.
- (12) Iversen, C.; Kjøniksen, A.-L.; Nyström, B.; Nakken, T.; Palmgren, O.; Tande, T. *Polym. Bull.* **1997**, *39*, 747.
- (13) Nyström, B.; Kjøniksen, A.-L.; Iversen, C. *Adv. Colloid Interface Sci.*, in press.
- (14) Roberts, G. A. F. *Chitin Chemistry*; MacMillan Press: Hong Kong, 1992.
- (15) Van Duin, P. J.; Hermans, J. J. *J. Polym. Sci.* **1959**, *36*, 295.
- (16) Roberts, G. A. F.; Domszy, J. G. *Int. J. Biol. Macromol.* **1982**, *4*, 374.
- (17) Muzzarelli, R. A. A.; Lough, C.; Emanuelli, M. *Carbohydr. Res.* **1987**, *164*, 433.
- (18) Delben, F.; Lapasin, R.; Pricl, S. *Int. J. Biol. Macromol.* **1990**, *12*, 9.
- (19) Matsumoto, T.; Kawai, M.; Masuda, T. *Biopolymers* **1991**, *31*, 1721.
- (20) Wang, W.; Qin, W.; Bo, S. *Makromol. Chem., Rapid Commun.* **1991**, *12*, 559.
- (21) Anthonen, M. W.; Vårum, K. M.; Smidsrød, O. *Carbohydr. Polym.* **1993**, *22*, 193.
- (22) Rinaudo, M.; Milas, M.; Dung, P. L. *Int. J. Biol. Macromol.* **1993**, *15*, 281.
- (23) Raymond, L.; Morin, F. G.; Marchessault, R. H. *Carbohydr. Res.* **1993**, *246*, 331.
- (24) Vårum, K. M.; Ottøy, M. H.; Smidsrød, O. *Carbohydr. Polym.* **1994**, *25*, 65.
- (25) Anthonen, M. W.; Vårum, K. M.; Hermansson, A. M.; Smidsrød, O.; Brant, D. A. *Carbohydr. Polym.* **1994**, *25*, 13.
- (26) Wu, C.; Zhou, S.; Wang, W. *Biopolymers* **1995**, *35*, 385.
- (27) Amiji, M. M. *Carbohydr. Polym.* **1995**, *26*, 211.
- (28) Ottøy, M. H.; Vårum, K. M.; Christensen, B. E.; Anthonen, M. W.; Smidsrød, O. *Carbohydr. Polym.* **1996**, *31*, 253.
- (29) Draget, K. I. *Polym. Gels Networks* **1996**, *4*, 143.
- (30) Mucha, M. *Macromol. Chem. Phys.* **1997**, *198*, 471.
- (31) Vårum, K. M.; Anthonen, M. W.; Grasdalen, H.; Smidsrød, O. *Carbohydr. Res.* **1991**, *211*, 17.
- (32) Moore, G. K.; Roberts, G. A. F. *Int. J. Biol. Macromol.* **1981**, *3*, 337.
- (33) Chu, B.; Onclin, M.; Ford, J. R. *J. Phys. Chem.* **1984**, *88*, 6566.
- (34) Guinier, A.; Fournet, G. *Small Angle Scattering of X-rays*; J. Wiley & Sons: New York, 1955.
- (35) Siegert, A. J. F. Massachusetts Institute of Technology, Rad. Lab. Rep. No. 465, 1943.
- (36) Nyström, B.; Roots, J.; Carlsson, A.; Lindman, B. *Polymer* **1992**, *33*, 2875.
- (37) Wang, C. H.; Zhang, X. Q. *Macromolecules* **1993**, *26*, 707.
- (38) Martin, J. E.; Wilcoxon, J.; Odinek, J. *Phys. Rev. A* **1991**, *43*, 858.
- (39) Nyström, B.; Walderhaug, H.; Hansen, F. K. *J. Phys. Chem.* **1993**, *97*, 7743.
- (40) Raspau, E.; Lairez, D.; Adam, M.; Carton, J.-P. *Macromolecules* **1994**, *27*, 2956.
- (41) Douglas, J. F.; Hubbard, J. B. *Macromolecules* **1991**, *24*, 3163.
- (42) Ngai, K. L. *Adv. Colloid Interface Sci.* **1996**, *64*, 1.
- (43) De Gennes, P.-G. *Scaling Concepts in Polymer Physics*; Cornell University Press: Ithaca, NY, 1979.
- (44) Daoud, M.; Leibler, L. *Macromolecules* **1988**, *21*, 1497.
- (45) Daoud, M.; Martin, J. E. In *The Fractal Approach to Heterogeneous Chemistry*; Avnir, D., Ed.; John Wiley & Sons: New York, 1989.
- (46) Muthukumar, M. *Macromolecules* **1989**, *22*, 4656.
- (47) Martin, J. E.; Wilcoxon, J. P. *Phys. Rev. A* **1989**, *39*, 252.
- (48) Förster, S.; Schmidt, M.; Antonietti, M. *Polymer* **1990**, *31*, 781.
- (49) Sedláč, M.; Amis, E. J. *J. Chem. Phys.* **1992**, *96*, 817.
- (50) Tanahatoe, J. J.; Kuil, M. E. *J. Phys. Chem. B* **1997**, *101*, 9233.
- (51) Adam, M.; Delsanti, M.; Munch, J. P.; Durand, D. *Phys. Rev. Lett.* **1988**, *61*, 706.
- (52) Ren, S. Z.; Shi, W. F.; Zhang, W. B.; Sorensen, C. M. *Phys. Rev. A* **1992**, *45*, 2416.
- (53) Sun, T.; King, H. E., Jr. *Macromolecules* **1996**, *29*, 3175.